Pergamon

0022–5096(94)00072–7

SHEAR DOMINATED TRANSONIC INTERFACIAL CRACK GROWTH IN A BIMATERIAL—II. ASYMPTOTIC FIELDS AND FAVORABLE VELOCITY REGIMES

CHENG LIU,† Y. HUANG‡ and ARES J. ROSAKIS

Graduate Aeronautical Laboratories, MS 105-50, California Institute of Technology, Pasadena, CA 91125, U.S.A.

ABSTRACT

Motivated by experimental observations of transonic crack tip speeds (Lambros and Rosakis, 1994c, *J. Mech. Phys. Solids* **43**(2), 169–188), the problem of intersonic interfacial crack growth in an elastic–rigid bimaterial system is analysed. Following the analytical procedure employed in Liu *et al.* (1993, *J. Mech. Phys. Solids* **41**, 1887–1954), the two-dimensional in-plane asymptotic deformation field surrounding the tip of a crack propagating intersonically along an elastic–rigid bimaterial interface, is obtained. The theoretical results show that the near-tip stress field does not exhibit oscillations, while a stress singularity weaker than 0.5 still exists and is a function of the crack tip speed. In addition, due to the intersonic nature of crack growth, a singular line emanating from the moving crack tip is present in the near-tip field. Across this line, stresses and particle velocities suffer infinite jumps. The theoretical analysis also shows that the near-tip deformation field is shear dominated. It is also shown that in the velocity range $c_s < v < \sqrt{2}c_s$, either crack face contact or negative normal tractions ahead of the crack tip exist. Visual evidence of such contact is reported in Part I of this study. These observations, together with additional experimental results of Part I, lead to the conclusion that crack growth is favorable in the velocity regimes $0 < v < c_s$ and $\sqrt{2}c_s < v < c_l$.

1. INTRODUCTION

Recent experimental studies, reported in Part I of this work (Lambros and Rosakis, 1994c), as well as in Liu *et al.* (1993), on the problem of dynamic interfacial fracture, have shown some surprising physical phenomena. Lambros and Rosakis (1994a, b), for example, observed that under certain loading conditions, the speed of a dynamically propagating interfacial crack in a bimaterial system, may exceed both the Rayleigh and the shear wave speeds of the more compliant of the two constituents. These observations are somewhat contradictory to previously speculated theoretical predictions. In the past, Atkinson (1977) claimed that the terminal speed of an interfacial crack should be the lower of the two Rayleigh wave speeds of the constituents of the bimaterial system, while Willis (1973) argued that the terminal speed should be slightly larger than the lower Rayleigh wave speed. Until recently, there

† Current address: MST-5, MS-G755, Los Alamos National Laboratory, Los Alamos, NM 87545, U.S.A.

‡ Department of Aerospace and Mechanical Engineering, The University of Arizona, Tucson, AZ 85721, U.S.A.

was no experimental evidence to support either point. The work of Lambros and Rosakis (1994a,b) has provided such evidence. Unfortunately, the experimental observations of transonic interfacial crack growth made by Lambros and Rosakis (1994a,b), could not be interpreted using the existing analytical results, which are only limited to the subsonic crack propagation regime.

A linearly elastic analysis of a transonically growing crack in a homogeneous solid (see Broberg, 1994) has shown that the energy release rate at the tip of a dynamically propagating mode-I crack, is always zero, no matter what the speed of propagation (as long as the crack tip speed exceeds c_s, the shear wave speed of the solid). In contrast, for a dynamically propagating mode-II crack, there is one particular velocity, $\sqrt{2}c_s$, where the energy release rate is finite. This would seem to imply that, if at all possible, transonic crack growth in homogeneous solids would occur at a velocity of $\sqrt{2}c_s$ and under mode-II conditions. This is of importance to geophysics where rupture of earthquake faults is always related to high speed propagation of shear cracks. For this reason, most dynamic fracture studies associated with fault rupture concentrate on mode-II crack propagation (Freund, 1979; Burridge *et al.*, 1979). In the work of Freund (1979), the asymptotic near-tip field for a shear crack growing transonically in a homogeneous material was obtained. Burridge *et al.* (1979) also introduced a finite cohesive zone ahead of the shear crack tip to study the stability of rapid crack growth. By studying a mode-II crack growing intersonically at a constant speed of $\sqrt{2}c_s$, under a remote uniform shear load and by using integral transforms, Broberg (1994) was able to obtain the exact solution of the shear traction distribution ahead of the crack tip. Similar issues have been addressed by, among others, Brock (1977), Simonov (1983), Broberg (1985, 1989), Bykovtsev and Kramarovskii (1989), and Aleksandrov and Smetanin (1990).

For dynamic interfacial crack growth in bimaterial systems, previous theoretical studies mainly focused on the sub-Rayleigh propagation regime, i.e. crack tip speed lower than the Rayleigh wave speed of the more compliant constituent in the bimaterial system. Among others, Gol'dshtein (1967), Brock and Achenbach (1973), Willis (1971, 1973) and Atkinson (1977) have provided crack line solutions of particular dynamic fracture problems in bimaterial systems. Of particular interest to the present study is the subsonic dynamic analysis of Brock (1979) who considered the extension of a dynamic shear interfacial flaw involving crack face friction. In order to investigate the asymptotic spatial structure of the field surrounding the moving interfacial crack tip, Yang *et al.* (1991) and Wu (1991) obtained the most singular term of the steady state elastodynamic bimaterial crack tip fields. In addition, Deng (1992) obtained an asymptotic series representation of the stress field near the tip of a running interfacial crack in a bimaterial system under steady state conditions. The analysis of Liu *et al.* (1993) provided the higher order transient asymptotic stress field surrounding a moving interfacial crack tip. Moreover, in the same work, they also obtained the solution for the super-Rayleigh, subsonic interfacial crack growth regime, where the crack tip speed is between the Rayleigh and the lower shear wave speeds. Most recently, Yu and Yang (1994) obtained the near tip asymptotic stress field for an antiplane shear (mode-III) propagating crack running at a speed between shear wave speeds of the constituents of the bimaterial interface.

Motivated by the above mentioned recent experimental studies, in this paper, the

problem of transonic interfacial crack growth in a bimaterial system will be analysed and the two-dimensional in-plane asymptotic deformation field surrounding the crack tip will be obtained. The method used to solve this problem follows the procedure employed in Liu et al. (1993). The results of the current theoretical analysis have been correlated with the experimental observations reported in Part I of this series (Lambros and Rosakis, 1994c) and results of the comparison were presented in Section 3.2 of Part I.

2. SUBSONIC, SUPER-RAYLEIGH INTERFACIAL CRACK GROWTH IN A BIMATERIAL SYSTEM

In homogeneous materials, an infinite amount of energy has to be transmitted to the crack tip to maintain crack extension at the Rayleigh wave speed if the dynamic stress intensity factor is to remain finite (Freund, 1990). This makes it impossible for a crack in a homogeneous solid to exceed the Rayleigh wave speed of that material. However, for a crack growing along a bimaterial interface, it has been shown that as the crack tip speed approaches the lower Rayleigh wave speed, $c_R^{(1)}$, only a finite amount of energy has to be transmitted to the crack tip if the dynamic stress intensity factor is to remain finite (see Yang et al., 1991). Accordingly, there is no energetic restriction for an interfacial crack to exceed the lower Rayleigh wave speed. The solution for subsonic, super-Rayleigh interfacial crack growth in a bimaterial system composed of two homogeneous, isotropic and linearly elastic solids, has been obtained by Liu et al. (1993). They observed that the governing equations for a dynamic crack growing along a bimaterial interface, remain elliptic for crack tip speeds in the range $0 < v < c_s^{(1)}$. Therefore, their general solution for the interfacial crack tip speed in the sub-Rayleigh regime, can be directly extended to the subsonic, super-Rayleigh regime. The results of their work are summarized below.

Suppose the properties of the materials constituting the interface are such that $c_s^{(1)} < c_R^{(2)}$, and the crack tip speed is in the range $c_R^{(1)} < v < c_s^{(1)}$. The oscillatory index parameter ε, which depends on the interfacial crack tip speed and the properties of the bimaterial combination, becomes complex and is given by

$$\varepsilon = \overset{*}{\varepsilon} + \tfrac{1}{2}i, \quad \overset{*}{\varepsilon} = \frac{1}{2\pi} \ln \frac{\beta - 1}{\beta + 1}, \tag{2.1}$$

where β is the second Dundur's parameter and also depends on the interfacial crack tip speed and the properties of the bimaterial combination. If only the leading term in the asymptotic expansion is considered, under the requirement of bounded displacement, or integrable mechanical energy density (Freund, 1990), in a coordinate system (η_1, η_2) translating with the moving crack tip, the first invariant of stress for the material above the interface was obtained as

$$\sigma_{11} + \sigma_{22} = \frac{4(\alpha_l^2 - \alpha_s^2) A(t)}{D(v) \sinh \overset{*}{\varepsilon} \pi} \left\{ 2\eta \alpha_s \cosh [\overset{*}{\varepsilon}(\pi - \theta_1)] \atop - (1 + \alpha_s^2) \sinh [\overset{*}{\varepsilon}(\pi - \theta_1)] \right\} \cos(\overset{*}{\varepsilon} \ln r_1 + \Phi(t)), \tag{2.2}$$
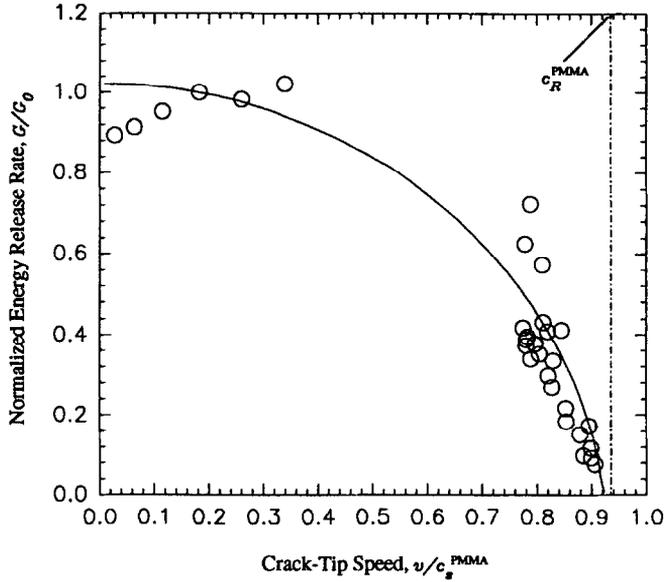
where

Fig. 1. Experimentally measured variation of energy release rate at the crack tip in the PMMA/4340 steel bimaterial system as a function of crack tip velocity (Lambros and Rosakis, 1994c).

$$\alpha_{l,s} = \left\{1 - \frac{v^2}{c_{l,s}^2}\right\}^{1/2}, \quad D(v) = 4\alpha_l^2\alpha_s - (1+\alpha_s^2)^2,$$

and the scaled polar coordinates (r_1, θ_1) are defined by

$$r_1 = (\eta_1^2 + \alpha_1\eta_2^2)^{1/2}, \quad \theta_1 = \tan^{-1}\frac{\alpha_1\eta_2}{\eta_1}.$$

For material-2 below the interface, we need only change the corresponding material parameters in (2.2) and replace $\overset{*}{\varepsilon}$ by $-\overset{*}{\varepsilon}$. In (2.2), $A(t)$ and $\Phi(t)$ are two real functions that can only be determined by the far field loading and geometry for each specific problem. It can be observed from (2.2) that oscillations in the stress field still exist along the radial direction. However, there is no singularity at the propagating crack tip. Since both stress and strain are bounded, the energy release rate at the tip of an interfacial crack whose speed is in the subsonic, super-Rayleigh range, will always be zero. In the experimental investigations reported in Lambros and Rosakis (1994b), it was found that the energy release rate at the crack tip decreases to zero as the speed of the interfacial crack approaches the lower Rayleigh wave speed of the bimaterial system. The variation of the normalized energy release rate as a function of crack tip speed is shown in Fig. 1.

3. TRANSONIC CRACK GROWTH ALONG THE INTERFACE BETWEEN AN ELASTIC SOLID AND A RIGID SUBSTRATE

In this section, we will study a special bimaterial system, namely one composed of a linearly elastic solid bonded to a rigid substrate. This problem approximates the
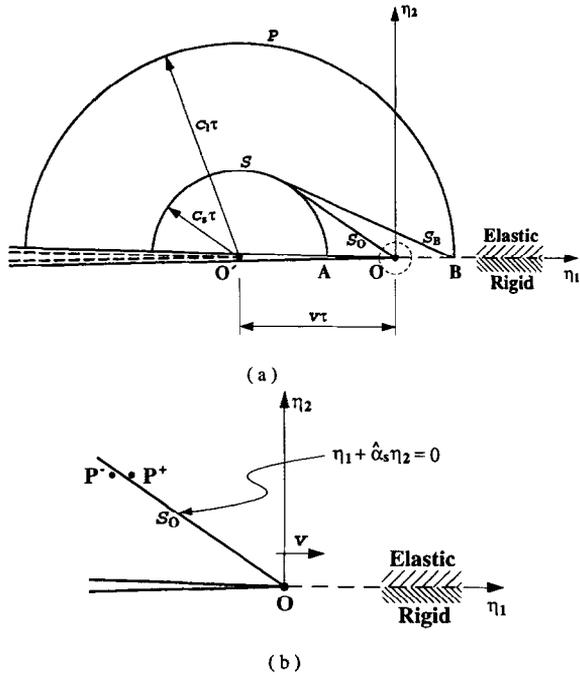
Fig. 2. A crack propagating intersonically along the interface of an elastic–rigid bimaterial system; (a) stress wave patterns, (b) detail of the near-tip region.

situation encountered in the PMMA/4340 steel bimaterial specimen described in Part I of this investigation where material mismatch is very close to the elastic–rigid model. The elastic–rigid approximation employed here involves a limitation that should be emphasized. In particular, the model cannot handle issues relating to energy transmission across the interface. However, the approximation made allows us to obtain concise analytical expressions that can be investigated to reveal some unique features of the near-tip stress fields.

Consider a bimaterial system composed of a homogeneous, isotropic and linearly elastic solid bonded to a rigid substrate. A crack propagates along the interface with velocity v. Let c_l and c_s be the longitudinal and shear wave speeds of the elastic material, respectively. The speed of the crack tip, v, is such that

$$c_s < v < c_l,$$

i.e. the crack propagates along the interface intersonically. Debonding beyond the longitudinal wave speed of the elastic material is not considered here. Figure 2(a) shows the propagation of wave fronts in the elastic medium as fracture initiates and proceeds along the interface. At some time in its propagation history, the crack tip was at position O'. After a time period τ, the crack tip moves to point O. Because of material rupture, stress waves will radiate into the elastic solid above the interface, while no wave propagation is possible in the lower constituent because it is rigid. The dilatational and shear wave fronts are centered at point O' and radiate into the elastic material. They are denoted by P and S in Fig. 2(a). Note that since $v > c_s$, the crack

tip has exceeded the shear wave emitted at point O'. However, ahead of the moving crack tip and behind the dilatational wave front P, a head wave region is generated and is denoted by S_B in Fig. 2(a). This head wave is necessary to ensure that the components of displacement vanish along the interface. In addition, ahead of the shear wave front S and behind the moving crack tip, the crack faces must remain traction free. Therefore, another head wave region is generated as well and is denoted by S_O. The head wave fronts S_B and S_O move with the shear wave speed c_s of the elastic material. Close to the moving crack tip within the area surrounded by the dotted circle, two different regions can be identified. These are seen in detail in Fig. 2(b). The region on the left of S_O has been affected by the head wave S_O. The one on the right has not experienced the deformation associated with S_O yet. This feature is distinct from that in the subsonic crack growth case, where complete information about the motion of the crack tip always reaches the points on the prospective crack path before the tip itself does.

For planar deformation, in a fixed coordinate system (x_1, x_2), the two components of the displacement field $u_\alpha(x_1, x_2, t)$, can be expressed in terms of two displacement potentials $\phi(x_1, x_2, t)$ and $\psi(x_1, x_2, t)$ through

$$u_\alpha(x_1, x_2, t) = \phi_{,\alpha}(x_1, x_2, t) + e_{\alpha\beta}\psi_{,\beta}(x_1, x_2, t), \tag{3.1}$$

where α, $\beta \in \{1, 2\}$ and the summation convention is employed here. $e_{\alpha\beta}$ are the components of the two-dimensional alternator, defined by

$$e_{12} = -e_{21} = 1, \quad e_{11} = e_{22} = 0.$$

The equation of motion that $\phi(x_1, x_2, t)$ satisfies is

$$\nabla^2 \phi(x_1, x_2, t) = \ddot{\phi}(x_1, x_2, t), \tag{3.2}$$

where ∇^2 is the Laplace operator, and $\{\cdot\}$ stands for a time derivative. The displacement potential $\psi(x_1, x_2, t)$ is composed of two parts $\psi_\beta(x_1, x_2, t)$, $\beta \in \{1, 2\}$. $\psi_1(x_1, x_2, t)$ is associated with the head wave S_O, generated by the transonic crack growth, while $\psi_2(x_1, x_2, t)$ is associated with the head wave S_B, linked with the propagation of the dilatational wave P along the interface. Both $\psi_1(x_1, x_2, t)$ and $\psi_2(x_1, x_2, t)$ satisfy the equation

$$\nabla^2 \psi_\beta(x_1, x_2, t) = \ddot{\psi}_\beta(x_1, x_2, t), \quad \beta \in \{1, 2\}. \tag{3.3}$$

Very close to the moving crack tip, or at "long" times after crack initiation, steady state conditions are expected to be established. As a result, in the moving coordinate system (η_1, η_2), the equations of motion take the form

$$\left.\begin{aligned}
\phi_{,11}(\eta_1, \eta_2) + \frac{1}{\alpha_l^2}\phi_{,22}(\eta_1, \eta_2) &= 0 \\[2mm]
\psi_{\beta,11}(\eta_1, \eta_2) - \frac{1}{\hat{\alpha}_s^2}\psi_{\beta,22}(\eta_1, \eta_2) &= 0
\end{aligned}\right\}, \quad \forall \eta_2 > 0, \quad \beta \in \{1, 2\}, \tag{3.4}$$

where

$$\alpha_1 = \left(1 - \frac{v^2}{c_1^2}\right)^{1/2}, \quad \hat{\alpha}_s = \left(\frac{v^2}{c_s^2} - 1\right)^{1/2}.$$

The above equations are the ones governing the steady state intersonic problem under consideration here. The first of equations (3.4), is elliptic while the second is hyperbolic. As a result, the most general solutions for $\phi(\eta_1,\eta_2)$ and $\psi_\beta(\eta_1,\eta_2)$ can be expressed by

$$\left.\begin{array}{l}\phi(\eta_1,\eta_2) = \mathrm{Re}\{F(z_1)\} \\ \psi_\beta(\eta_1,\eta_2) = g_\beta(\eta_1 + \hat{\alpha}_s\eta_2) + \overset{*}{g}_\beta(\eta_1 - \hat{\alpha}_s\eta_2)\end{array}\right\}, \quad \forall \eta_2 > 0, \quad \beta \in \{1,2\}, \quad (3.5)$$

where $z_1 = \eta_1 + i\alpha_1\eta_2$, and $F(z_1)$ is an analytic function of z_1 in the upper half plane. $g_\beta(\eta_1 + \hat{\alpha}_s\eta_2)$ and $\overset{*}{g}_\beta(\eta_1 - \hat{\alpha}_s\eta_2)$ are real functions of their respective arguments. Since to the right of the head wave region S_O, material particles have not felt the disturbance caused by crack growth yet, we can introduce the following restrictions to $g_1(\eta_1 + \hat{\alpha}_s\eta_2)$ and $\overset{*}{g}_1(\eta_1 - \hat{\alpha}_s\eta_2)$,

$$\left.\begin{array}{l}\overset{*}{g}_1(\eta_1 - \hat{\alpha}_s\eta_2) = 0, \quad -\infty < \eta_1 < \infty, \eta_2 > 0 \\ g_1(\eta_1 + \hat{\alpha}_s\eta_2) = 0, \quad \text{for } \eta_1 + \hat{\alpha}_s\eta_2 > 0\end{array}\right\}. \quad (3.6)$$

On the other hand, as $\eta_1 - \hat{\alpha}_s\eta_2 \to \infty$, the disturbance of the head wave S_B has not been felt by the material particles, see Fig. 2(a), therefore

$$\overset{*}{g}_2(\eta_1 - \hat{\alpha}_s\eta_2) = 0, \quad -\infty < \eta_1 < \infty, \eta_2 > 0. \quad (3.7)$$

Based on the above observations, the steady state displacement potential $\psi(\eta_1,\eta_2)$ which is a combination of $\psi_1(\eta_1,\eta_2)$ and $\psi_2(\eta_1,\eta_2)$, acquires the form

$$\psi(\eta_1,\eta_2) = g(\eta_1 + \hat{\alpha}_s\eta_2), \quad \forall \eta_2 > 0, \quad (3.8)$$

where $g(\eta_1 + \hat{\alpha}_s\eta_2)$ is a real function of its argument.

For the elastic material above the interface, we can express the components of displacement as

$$\left.\begin{array}{l}u_1 = \mathrm{Re}\{F'(z_1)\} + \hat{\alpha}_s g'(\eta_1 + \hat{\alpha}_s\eta_2) \\ u_2 = -\alpha_1\mathrm{Im}\{F'(z_1)\} - g'(\eta_1 + \hat{\alpha}_s\eta_2)\end{array}\right\}, \quad \forall \eta_2 > 0, \quad (3.9)$$

and the components of stress as

$$\left.\begin{array}{l}\sigma_{11} = \mu\{(1 + 2\alpha_1^2 + \hat{\alpha}_s^2)\,\mathrm{Re}\{F''(z_1)\} + 2\hat{\alpha}_s g''(\eta_1 + \hat{\alpha}_s\eta_2)\} \\ \sigma_{22} = -\mu\{(1 - \hat{\alpha}_s^2)\,\mathrm{Re}\{F''(z_1)\} + 2\hat{\alpha}_s g''(\eta_1 + \hat{\alpha}_s\eta_2)\} \\ \sigma_{12} = -\mu\{2\alpha_1\mathrm{Im}\{F''(z_1)\} + (1 - \hat{\alpha}_s^2)\,g''(\eta_1 + \hat{\alpha}_s\eta_2)\}\end{array}\right\}, \quad \forall \eta_2 > 0, \quad (3.10)$$

where a prime denotes a derivative with respect to the corresponding argument and μ is the shear modulus of the elastic material.

Introduce now the following notation:

$$\lim_{\eta_2 \to 0^{\pm}} \Omega(z) = \Omega^{\pm}(\eta_1), \quad z = \eta_1 + i\eta_2.$$

For $\eta_1 < 0$ and $\eta_2 \to 0^+$, the traction free condition on the upper crack face demands

$$\sigma_{22}(\eta_1, 0^+, t) = \sigma_{12}(\eta_1, 0^+, t) = 0,$$

or, in terms of $F(z_i)$ and $g(\eta_1 + \hat{\alpha}_s \eta_2)$,

$$\left. \begin{aligned} (1 - \hat{\alpha}_s^2)\{F''^+(\eta_1) + \bar{F}''^-(\eta_1)\} + 4\hat{\alpha}_s g''(\eta_1) = 0 \\ \alpha_1\{F''^+(\eta_1) - \bar{F}''^-(\eta_1)\} + i(1 - \hat{\alpha}_s^2) g''(\eta_1) = 0 \end{aligned} \right\}, \quad \forall \eta_1 < 0, \tag{3.11}$$

where the notation $\bar{F}(\cdot)$ stands for the complex conjugate of the analytic function $F(\cdot)$. Along the interface, i.e. $\eta_1 > 0$, $\eta_2 = 0$, the components of displacement should vanish since the elastic material is bonded to a rigid substrate. As a result, we have

$$\left. \begin{aligned} F'^+(\eta_1) + \bar{F}'^-(\eta_1) + 2\hat{\alpha}_s g'(\eta_1) = 0 \\ \alpha_1\{F'^+(\eta_1) - \bar{F}'^-(\eta_1)\} + 2i g'(\eta_1) = 0 \end{aligned} \right\}, \quad \forall \eta_1 > 0. \tag{3.12}$$

By eliminating $g(\eta_1)$ from (3.11) and (3.12), we can obtain equations involving only the analytic function $F(z)$, i.e.

$$F''^+(\eta_1) - \frac{4\alpha_1\hat{\alpha}_s + i(1 - \hat{\alpha}_s^2)^2}{4\alpha_1\hat{\alpha}_s - i(1 - \hat{\alpha}_s^2)^2} \bar{F}''^-(\eta_1) = 0, \quad \forall \eta_1 < 0, \tag{3.13}$$

and

$$F'^+(\eta_1; t) - \frac{\alpha_1\hat{\alpha}_s + i}{\alpha_1\hat{\alpha}_s - i} \bar{F}'^-(\eta_1; t) = 0, \quad \forall \eta_1 > 0. \tag{3.14}$$

From (3.14) and by using analytic continuation, we may introduce a new function $\theta(z)$ as follows:

$$\left. \begin{aligned} \theta(z) = (\alpha_1\hat{\alpha}_s - i) F'(z), \quad z \in S^+ \\ \theta(z) = (\alpha_1\hat{\alpha}_s + i) \bar{F}'(z), \quad z \in S^- \end{aligned} \right\}, \tag{3.15}$$

where

$$S^{\pm} = \begin{cases} \{(\eta_1, i\eta_2) \mid -\infty < \eta_1 < \infty, \eta_2 \geqslant 0\} - C \\ \{(\eta_1, i\eta_2) \mid -\infty < \eta_1 < \infty, \eta_2 \leqslant 0\} - C, \end{cases}$$

$$C = \{(\eta_1, i\eta_2) \mid -\infty < \eta_1 \leqslant 0, \eta_2 = 0\}.$$

In terms of the new analytic function $\theta(z)$, (3.13) can be rewritten as

$$\theta'^+(\eta_1) - e^{-2i\beta(v)} \theta'^-(\eta_1) = 0, \quad \forall \eta_1 < 0, \tag{3.16}$$

where

$$\beta(v) = \tan^{-1} \frac{\alpha_1\hat{\alpha}_s\{4 - (1 - \hat{\alpha}_s^2)^2\}}{4\alpha_1^2\hat{\alpha}_s^2 + (1 - \hat{\alpha}_s^2)^2}.$$
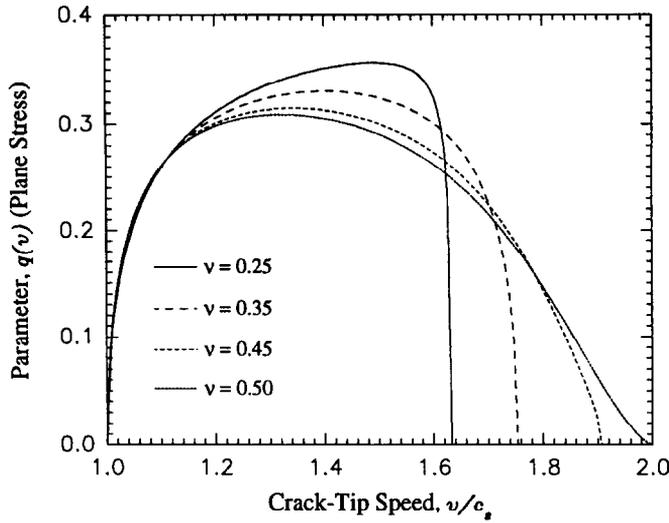
Fig. 3. Variation of the singularity exponent $q(v)$ as a function of the crack tip speed v for different values of Poisson's ratio.

Equation (3.16) constitutes a Riemann–Hilbert problem. Its solution $\theta'(z)$ is analytic in the cut-plane $S^+ \cup S^-$. Along the cut C, $\theta'(z)$ satisfies (3.16). Also, from the requirement of bounded displacements at the crack tip, as $|z| \to 0$,

$$|\theta'(z)| = O(|z|^\alpha), \tag{3.17}$$

for some $\alpha > -1$. The solution to (3.16) can be written as

$$\theta'(z) = \frac{A(z)}{z^{q(v)}}, \tag{3.18}$$

where $A(z)$ is an arbitrary entire function. The exponent $q(v)$ is a function that depends on the crack tip speed v and Poisson's ratio v. $q(v)$ is given by

$$q(v) = \frac{1}{\pi} \tan^{-1} \frac{\alpha_l \hat{\alpha}_s \{4 - (1 - \hat{\alpha}_s^2)^2\}}{4 \alpha_l^2 \hat{\alpha}_s^2 + (1 - \hat{\alpha}_s^2)^2}. \tag{3.19}$$

The variation of $q(v)$ with crack tip speed v is plotted in Fig. 3 for different values of Poisson's ratio of the elastic material. It should be noted at this point that $q(v)$ remains less than 0.5 for the entire velocity range considered in this paper.

Returning to (3.15), it is obvious that

$$\left. \begin{array}{ll} F''(z) = \dfrac{1}{\alpha_l \hat{\alpha}_s - i} \cdot \dfrac{A(z)}{z^{q(v)}}, & z \in S^+ \\[2ex] \bar{F}''(z) = \dfrac{1}{\alpha_l \hat{\alpha}_s + i} \cdot \dfrac{A(z)}{z^{q(v)}}, & z \in S^- \end{array} \right\}, \tag{3.20}$$

which reveals that the undetermined entire function $A(z)$ has the property

$$\bar{A}(z) = A(z),$$

or in other words, if $A(z)$ is expanded into Taylor series,

$$A(z) = \sum_{n=0}^{\infty} A_n z^n,$$

then all coefficients $A_n (n = 1, 2, \ldots)$ are real.

From (3.11) and (3.12), the real function $g(\eta_1)$ can be determined for either $\eta_1 > 0$, or $\eta_1 < 0$. Finally, the leading terms of the two steady state displacement potentials $\phi(\eta_1, \eta_2)$ and $\psi(\eta_1, \eta_2)$ are given by

$$
\phi(\eta_1, \eta_2) = \frac{1}{1 + \alpha_1^2 \hat{\alpha}_s^2} \cdot \frac{A_0}{(2 - q(v))(1 - q(v))} \cdot \frac{1}{r_1^{q(v) - 2}}
$$
$$
\times \{\alpha_1 \hat{\alpha}_s \cos(2 - q(v))\theta_1 - \sin(2 - q(v))\theta_1\}
$$

$$
\psi(\eta_1, \eta_2) = -\frac{1}{1 + \alpha_1^2 \hat{\alpha}_s^2} \cdot \frac{A_0}{(2 - q(v))(1 - q(v))}
$$
$$
\times \left\{ \frac{\alpha_1}{(\eta_1 + \hat{\alpha}_s \eta_2)^{q(v) - 2}} H(\eta_1 + \hat{\alpha}_s \eta_2) \right.
$$
$$
\left. + \frac{1 - \hat{\alpha}_s^2}{2\hat{\alpha}_s} \cdot \frac{\alpha_1 \hat{\alpha}_s \cos \pi q(v) + \sin \pi q(v)}{(-\eta_1 - \hat{\alpha}_s \eta_2)^{q(v) - 2}} H(-\eta_1 - \hat{\alpha}_s \eta_2) \right\}, \qquad (3.21)
$$

where $H(\cdot)$ is the Heaviside step function and the scaled polar coordinates (r_1, θ_1) are given by

$$
r_1 = \sqrt{\eta_1^2 + \alpha_1^2 \eta_2^2}, \quad \theta_1 = \tan^{-1} \frac{\alpha_1 \eta_2}{\eta_1}.
$$

By using the above expressions for $\phi(\eta_1, \eta_2)$ and $\psi(\eta_1, \eta_2)$, the displacement field in the elastic solid can be computed as

$$
u_1 = \frac{1}{1 + \alpha_1^2 \hat{\alpha}_s^2} \cdot \frac{A_0}{1 - q(v)} \left\{ \frac{1}{r_1^{q(v) - 1}} [\alpha_1 \hat{\alpha}_s \cos(1 - q(v))\theta_1 - \sin(1 - q(v))\theta_1] \right.
$$

$$
- \frac{\alpha_1 \hat{\alpha}_s}{(\eta_1 + \hat{\alpha}_s \eta_2)^{q(v) - 1}} H(\eta_1 + \hat{\alpha}_s \eta_2)
$$

$$
\left. + \frac{1 - \hat{\alpha}_s^2}{2} \cdot \frac{\alpha_1 \hat{\alpha}_s \cos \pi q(v) + \sin \pi q(v)}{(-\eta_1 - \hat{\alpha}_s \eta_2)^{q(v) - 1}} H(-\eta_1 - \hat{\alpha}_s \eta_2) \right\}
$$

$$
u_2 = -\frac{1}{1 + \alpha_1^2 \hat{\alpha}_s^2} \cdot \frac{A_0}{1 - q(v)} \left\{ \frac{\alpha_1}{r_1^{q(v) - 1}} \cdot [\cos(1 - q(v))\theta_1 + \alpha_1 \hat{\alpha}_s \sin(1 - q(v))\theta_1] \right.
$$

$$
- \frac{\alpha_1}{(\eta_1 + \hat{\alpha}_s \eta_2)^{q(v) - 1}} H(\eta_1 + \hat{\alpha}_s \eta_2)
$$

$$+\frac{1-\hat{\alpha}_s^2}{2\hat{\alpha}_s}\cdot\frac{\alpha_1\hat{\alpha}_s\cos\pi q(v)+\sin\pi q(v)}{(-\eta_1-\hat{\alpha}_s\eta_2)^{q(v)-1}}H(-\eta_1-\hat{\alpha}_s\eta_2)\biggr\}. \tag{3.22}$$

The stress field in the elastic solid is

$$\sigma_{11}=\frac{\mu A_0}{1+\alpha_1^2\hat{\alpha}_s^2}\biggl\{\frac{1+2\alpha_1^2+\hat{\alpha}_s^2}{r_1^{q(v)}}[\alpha_1\hat{\alpha}_s\cos q(v)\theta_1+\sin q(v)\theta_1]$$

$$-\frac{2\alpha_1\hat{\alpha}_s}{(\eta_1+\hat{\alpha}_s\eta_2)^{q(v)}}H(\eta_1+\hat{\alpha}_s\eta_2)$$

$$-\frac{(1-\hat{\alpha}_s^2)(\alpha_1\hat{\alpha}_s\cos\pi q(v)+\sin\pi q(v))}{(-\eta_1-\hat{\alpha}_s\eta_2)^{q(v)}}H(-\eta_1-\hat{\alpha}_s\eta_2)\biggr\}$$

$$\sigma_{22}=-\frac{\mu A_0}{1+\alpha_1^2\hat{\alpha}_s^2}\biggl\{\frac{1-\hat{\alpha}_s^2}{r_1^{q(v)}}[\alpha_1\hat{\alpha}_s\cos q(v)\theta_1+\sin q(v)\theta_1]$$

$$-\frac{2\alpha_1\hat{\alpha}_s}{(\eta_1+\hat{\alpha}_s\eta_2)^{q(v)}}H(\eta_1+\hat{\alpha}_s\eta_2)$$

$$-\frac{(1-\hat{\alpha}_s^2)(\alpha_1\hat{\alpha}_s\cos\pi q(v)+\sin\pi q(v))}{(-\eta_1-\hat{\alpha}_s\eta_2)^{q(v)}}H(-\eta_1-\hat{\alpha}_s\eta_2)\biggr\}$$

$$\sigma_{12}=-\frac{\mu A_0}{1+\alpha_1^2\hat{\alpha}_s^2}\biggl\{\frac{2\alpha_1}{r_1^{q(v)}}[\cos q(v)\theta_1-\alpha_1\hat{\alpha}_s\sin q(v)\theta_1]$$

$$-\frac{\alpha_1(1-\hat{\alpha}_s^2)}{(\eta_1+\hat{\alpha}_s\eta_2)^{q(v)}}H(\eta_1+\hat{\alpha}_s\eta_2)$$

$$-\frac{(1-\hat{\alpha}_s^2)^2}{2\hat{\alpha}_s}\cdot\frac{\alpha_1\hat{\alpha}_s\cos\pi q(v)+\sin\pi q(v)}{(-\eta_1-\hat{\alpha}_s\eta_2)^{q(v)}}H(-\eta_1-\hat{\alpha}_s\eta_2)\biggr\}, \tag{3.23}$$

while the field of particle velocity is given by

$$v_1=-\frac{vA_0}{1+\alpha_1^2\hat{\alpha}_s^2}\biggl\{\frac{1}{r_1^{q(v)}}[\alpha_1\hat{\alpha}_s\cos q(v)\theta_1+\sin q(v)\theta_1]$$

$$-\frac{\alpha_1\hat{\alpha}_s}{(\eta_1+\hat{\alpha}_s\eta_2)^{q(v)}}H(\eta_1+\hat{\alpha}_s\eta_2)$$

$$-\frac{1-\hat{\alpha}_s^2}{2}\cdot\frac{\alpha_1\hat{\alpha}_s\cos\pi q(v)+\sin\pi q(v)}{(-\eta_1-\hat{\alpha}_s\eta_2)^{q(v)}}H(-\eta_1-\hat{\alpha}_s\eta_2)\biggr\}$$

$$v_2=\frac{vA_0}{1+\alpha_1^2\hat{\alpha}_s^2}\biggl\{\frac{\alpha_1}{r_1^{q(v)}}[\cos q(v)\theta_1-\alpha_1\hat{\alpha}_s\sin q(v)\theta_1]$$

$$-\frac{\alpha_1}{(\eta_1+\hat{\alpha}_s\eta_2)^{q(v)}}H(\eta_1+\hat{\alpha}_s\eta_2)$$

$$-\frac{1-\hat{\alpha}_s^2}{2\hat{\alpha}_s}\cdot\frac{\alpha_1\hat{\alpha}_s\cos\pi q(v)+\sin\pi q(v)}{(-\eta_1-\hat{\alpha}_s\eta_2)^{q(v)}}H(-\eta_1-\hat{\alpha}_s\eta_2)\bigg\}. \qquad (3.24)$$

4. DISCUSSION

In the previous section, we obtained the leading term of the asymptotic expansion governing the deformation field surrounding the tip of an interfacial crack propagating intersonically in an elastic–rigid bimaterial system. The key features of this field will be discussed in this section.

Across the head wave front S_O, see Fig. 2(b), the components of stress and particle velocity are discontinuous. The jump in these quantities can be derived as follows.

Let point $(\overset{*}{\eta}_1, \overset{*}{\eta}_2)$ be on the head wave front S_O, or equivalently,

$$\overset{*}{\eta}_1 + \hat{\alpha}_s \overset{*}{\eta}_2 = 0, \quad \overset{*}{\eta}_2 > 0.$$

Also let points $P^\pm$ be to the right and left of S_O, respectively. These points will have coordinates $(\overset{*}{\eta}_1 \pm \delta, \overset{*}{\eta}_2)$, where δ is an infinitesimal positive number. Define now the δ-jump of any field quantity ω across S_O by

$$[\omega]_\delta = \omega(\overset{*}{\eta}_1 + \delta, \overset{*}{\eta}_2) - \omega(\overset{*}{\eta}_1 - \delta, \overset{*}{\eta}_2).$$

Then, the respective δ-jumps of the particle velocity and stress components across S_O, are

$$\left.\begin{array}{c} [v_\alpha]_\delta = \dfrac{\overset{\circ}{v}_\alpha}{\delta^{q(v)}} \\[4mm] [\sigma_{\alpha\beta}]_\delta = \dfrac{\overset{\circ}{\sigma}_{\alpha\beta}}{\delta^{q(v)}} \end{array}\right\}, \quad \alpha, \beta \in \{1, 2\} \qquad (4.1)$$

where

$$\overset{\circ}{v}_1 = \tfrac{1}{2}vA_0L(v), \quad \overset{\circ}{v}_2 = -\frac{1}{2\hat{\alpha}_s}vA_0L(v),$$

and

$$\overset{\circ}{\sigma}_{11} = -\mu A_0 L(v), \quad \overset{\circ}{\sigma}_{22} = \mu A_0 L(v), \quad \overset{\circ}{\sigma}_{12} = \frac{1-\hat{\alpha}_s^2}{2\hat{\alpha}_s}\mu A_0 L(v).$$

The function $L(v)$ which depends on the crack tip speed, is given by

$$L(v) = \frac{2\alpha_1\hat{\alpha}_s - (1-\hat{\alpha}_s^2)(\alpha_1\hat{\alpha}_s\cos\pi q(v)+\sin\pi q(v))}{1+\alpha_1^2\hat{\alpha}_s^2}.$$

As $\delta \to 0$, the jumps in stress and particle velocity become unbounded. Therefore, unlike subsonic crack growth where only one singular point is present at the crack tip, for intersonic crack growth, an entire line of infinite jumps in stress and particle

velocity appears in the body. This line starts from the crack tip and radiates into the elastic solid. Each point on this line has the same singularity as the crack tip.

The expression for the energy flux $F(\Gamma)$ into the crack tip through a contour Γ has been provided by Freund (1972, 1990) and is given by

$$F(\Gamma) = \int_\Gamma \{\sigma_{\alpha\beta} n_\alpha v_\beta + (U+T) v n_1\} \, ds, \qquad (4.2)$$

where Γ is a small contour which begins from the lower crack surface, surrounds the crack tip, and ends on the upper crack surface. n_α are the Cartesian components of the outward unit normal of Γ. U and T are the densities of the strain energy and kinetic energy, respectively. In the definition of $F(\Gamma)$ given in (4.2), it has been assumed that the displacement field is smooth enough so that it has continuous second derivatives. However, in the present case, the smoothness requirement for displacement field is lost.

Following the definition given in Abeyaratne and Knowles (1990), the scalar driving traction $f(\overset{*}{\eta}_1, \overset{*}{\eta}_2)$ on the singular line S_O, $\overset{*}{\eta}_1 + \alpha_1 \overset{*}{\eta}_2 = 0$, can be expressed as

$$f(\overset{*}{\eta}_1, \overset{*}{\eta}_2) = [U(\overset{*}{\eta}_1, \overset{*}{\eta}_2)]_\delta - \tfrac{1}{2}\{\sigma_{\alpha\beta}(\overset{*}{\eta}_1 + \delta, \overset{*}{\eta}_2) + \sigma_{\alpha\beta}(\overset{*}{\eta}_1 - \delta, \overset{*}{\eta}_2)\}[\varepsilon_{\alpha\beta}(\overset{*}{\eta}_1, \overset{*}{\eta}_2)]_\delta, \quad (4.3)$$

where U is the elastic energy density and $[\cdot]_\delta$ is the δ-jump defined at the beginning of this section. By using the results obtained in the previous section, one can show that the driving traction on the singular line S_O vanishes. This implies that there is no energy dissipation when the singular line S_O moves through the material. As a result, the energy flux into the crack tip through a contour Γ in the presence of a discontinuous line radiating from the moving crack tip, is still given by (4.2).

By recalling that the parameter $q(v)$ given in (3.19) which characterizes the strength of the singularity, is always less than 0.5, see Fig. 3, the energy flux into the moving crack tip is always zero irrespective of crack tip velocity. It is believed that when a finite process zone is introduced at the transonically moving crack tip, the energy flux into the crack will not vanish. This has been shown for homogeneous materials by Broberg (1994), where he considered mode-II transonic crack growth in a homogeneous solid.

By using the results obtained in the previous section, the normal traction along the interface and at a distance a ahead of the moving crack tip, assumes the form,

$$\sigma_{22}(a, 0^+, t) = \frac{\alpha_1 \hat{\alpha}_s (1 + \hat{\alpha}_s^2)}{1 + \alpha_1^2 \hat{\alpha}_s^2} \cdot \frac{\mu A_0}{a^{q(v)}}. \qquad (4.4)$$

While the crack opening displacement at a distance a behind the moving crack tip is given by

$$u_2(-a, 0^+, t) = -\frac{(1 - \hat{\alpha}_s^2)\alpha_1(1 + \hat{\alpha}_s^2)}{4\alpha_1^2 \hat{\alpha}_s^2 + (1 - \hat{\alpha}_s^2)^2} \cdot \frac{\cos \pi q(v)}{1 - q(v)} A_0 a^{1 - q(v)}. \qquad (4.5)$$

As a result, one can show that

$$\sigma_{22}(a,0^+,t)u_2(-a,0^+,t) = -\left(2 - \frac{v^2}{c_s^2}\right)W(v)\mu A_0^2 a^{1-2q(v)}, \qquad (4.6)$$

where

$$W(v) = \frac{\alpha_l^2 \hat{\alpha}_s(1+\hat{\alpha}_s^2)^2}{(1+\alpha_l^2\hat{\alpha}_s^2)\{4\alpha_l^2\hat{\alpha}_s^2+(1-\hat{\alpha}_s^2)^2\}} \cdot \frac{\cos \pi q(v)}{1-q(v)}.$$

Since $W(v)$ is always positive, (4.6) implies that if the crack tip speed is in the range $c_s < v < \sqrt{2}c_s$, $\sigma_{22}(a,0^+,t)$ and $u_2(-a,0^+,t)$ have opposite signs. This means that when the normal traction ahead of the crack tip is positive, crack face penetration into the rigid substrate is predicted. Since penetration is physically impossible, this would imply that the crack faces will come into contact, a situation which has been experimentally observed in Part I of this investigation, see Fig. 7 of Part I. When this situation arises, the solution is no longer valid and the problem should be revisited under different crack face boundary conditions. Conversely, (4.6) also implies that if the crack opening displacement is positive, the traction ahead of the crack tip remains negative, a condition which does not facilitate rupture of the bond. However, when the crack tip speed is in the range $\sqrt{2}c_s < v < c_l$, both $\sigma_{22}(a,0^+,t)$ and $u_2(-a,0^+,t)$ have the same signs, i.e. a positive normal traction ahead of the crack tip induces crack opening behind the tip.

The above discussion suggests that the velocity range from c_s to $\sqrt{2}c_s$ is not favorable for stable intersonic interfacial crack propagation. This is consistent with experimental observations of Part I in which crack tip velocities seem to remain around c_s for some time and then quickly accelerate to values higher than $\sqrt{2}c_s$. A similar phenomenon has been observed by Andrews (1976) who numerically studied transonic shear crack propagation in a homogeneous solid. He found that as soon as the crack tip speed reaches the Rayleigh wave speed c_R of the material, it quickly increases to values larger than $\sqrt{2}c_s$. He concluded that crack growth is unstable in the range $c_R < v < \sqrt{2}c_s$ and preferable speeds for a shear crack growing in a homogeneous material are either those lower than the Rayleigh wave speed, or those in the range $\sqrt{2}c_s < v < c_l$.

The experimental observations reported in the first part of this study (Lambros and Rosakis, 1994c) have found that transonic crack growth in a PMMA/4340 steel bimaterial system is shear dominated. For the elastic–rigid combination considered here, the ratio of crack opening displacements δ_1/δ_2 is given by

$$\frac{\delta_1}{\delta_2} = \frac{u_1|_{r=a,\theta=\pi}}{u_2|_{r=a,\theta=\pi}} = \frac{2\hat{\alpha}_s}{1-\hat{\alpha}_s^2}. \qquad (4.7)$$

Figure 4 shows the variation of the ratio δ_1/δ_2 as a function of crack tip speed. In this figure, there are two branches for δ_1/δ_2. Along the first, dashed line, branch δ_2 is negative (contact) if positive opening tractions are to be sustained ahead of the crack tip. This corresponds to the regime where stable crack growth is unfavorable, as discussed above. The second, solid line, branch corresponds to the favorable regime. In this regime, the magnitude of δ_1/δ_2 is always greater than 1 which implies that the deformation is shear dominated. Therefore, our theoretical analysis also predicts that
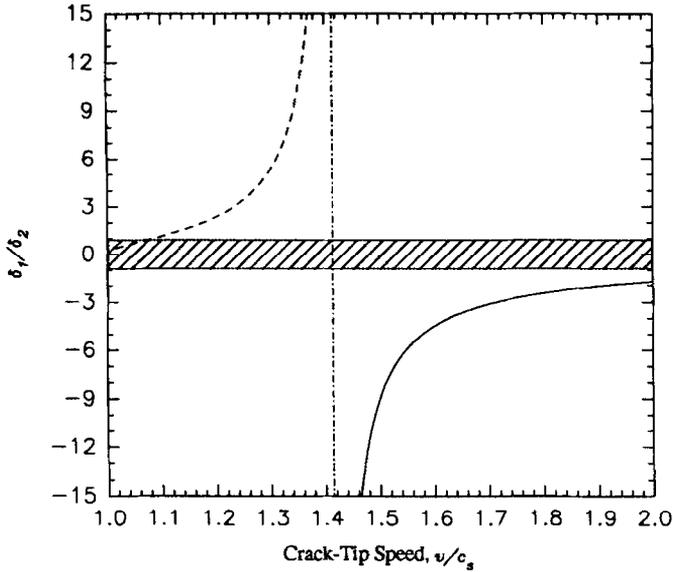
Fig. 4. Variation of the ratio of crack face displacements δ_1/δ_2 as a function of the interfacial crack tip speed.

the deformation field surrounding a transonically moving crack tip in a bimaterial system, will be predominantly shear. Transonic crack growth in a predominantly opening deformation field cannot be sustained. This is consistent with the experimental observations reported in Part I of this study and the previous results of Andrews (1976).

Finally, by using the results given in the previous section, the x_1-gradient of the first stress invariant can be expressed by

$$(\sigma_{11} + \sigma_{22})_{,1} = -\frac{2\mu A_0}{r_l^{q(v)+1}} \cdot \frac{q(v)(\alpha_l^2 + \hat{\alpha}_s^2)}{1 + \alpha_l^2 \hat{\alpha}_s^2} \{\alpha_l \hat{\alpha}_s \cos(q(v)+1)\theta_l + \sin(q(v)+1)\theta_l\}. \quad (4.8)$$

The optical interferometer CGS provides contours of this quantity. We can therefore, synthetically produce a CGS fringe pattern using (4.8). For a bimaterial system composed of PMMA bonded to a rigid substrate, a simulated CGS fringe pattern is shown in Fig. 5. Here, a Poisson's ratio of $v = 0.35$ has been used, and the crack tip speed is chosen as $v = 1.50c_s$. We can see that the fringe pattern shown in Fig. 5, resembles the qualitative features of the patterns obtained in experiments (see Fig. 4 of Part I), i.e. the fringes are squeezed in the crack propagation direction and are elongated in the direction normal to the crack.

5. CONCLUDING REMARKS

In the present study, we obtained the asymptotic deformation field surrounding the tip of a crack propagating transonically along the interface of an elastic–rigid bi-
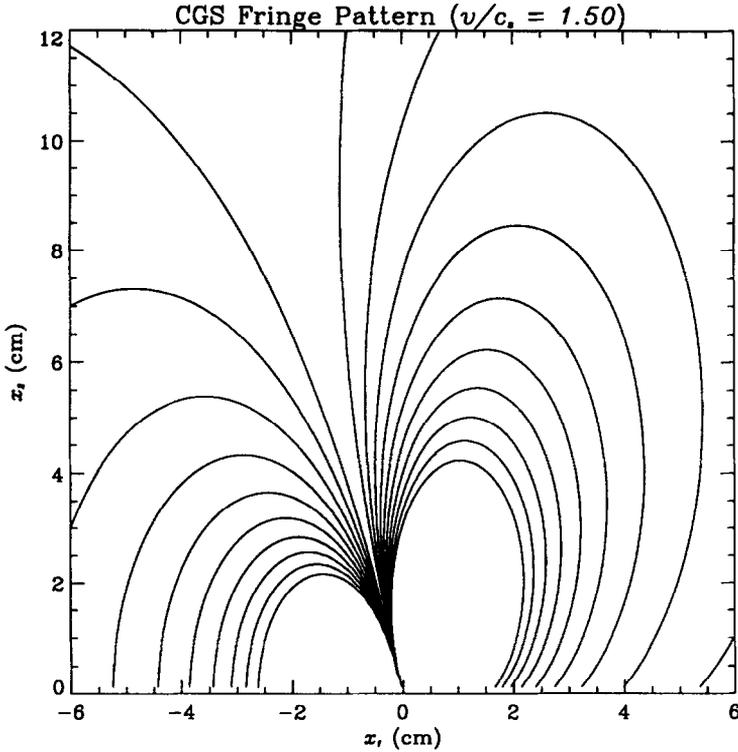
Fig. 5. Simulated CGS fringe pattern.

material system. We found that in contrast to subsonic crack growth in bimaterial systems, the near-tip stress field does not exhibit oscillations. However, a stress singularity still exists and is a function of the crack tip speed. In addition, we found that an entire singular line is present in the near-tip field. This singular line radiates from the crack tip and moves with it. Across the line, components of stress and particle velocity suffer infinite jumps. The energy release rate at the moving crack tip is found to be zero because the singularity is always less than $1/2$. The theoretical analysis has shown that in the velocity range $c_s < v < \sqrt{2}c_s$, either crack face contact or negative normal tractions ahead of the crack tip is predicted. This intuitively implies that this velocity regime is unfavorable for stable crack growth. For $\sqrt{2}c_s < v < c_l$, this situation does not arise. This is consistent with experimental observations in PMMA/4340 steel bimaterial specimens where the interfacial crack tip speed quickly accelerates from the shear wave speed of PMMA to values larger than $\sqrt{2}c_s^{PMMA}$. The theoretical analysis predicts that the near-tip deformation field for transonic crack growth is predominantly of a shear nature. This has also been confirmed by experimental investigations reported in the first part of this study (Lambros and Rosakis, 1994c).

ACKNOWLEDGEMENTS

REFERENCES

Abeyaratne, R. and Knowles, J. K. (1990) On the driving traction acting on a surface of strain discontinuity in a continuum. *J. Mech. Phys. Solids* **38**(3), 345–360.

Aleksandrov, V. M. and Smetanin, B. I. (1990) Supersonic cleavage of an elastic strip. *Appl. Math. Mech.* **54**(5), 677–682.

Andrews, D. J. (1976) Rupture velocity of plane strain shear cracks. *J. Geophys. Res.* **81**, 5679–5687.

Atkinson, C. (1977) Dynamic crack problems in dissimilar media. *Mechanics of Fracture*, Vol. 4 (ed. G. C. Sih), pp. 213–248. Noordhoff, Leyden, The Netherlands.

Broberg, K. B. (1985) Irregularities at earthquake slip. *J. Tech. Phys.* **26**(3–4), 275–284.

Broberg, K. B. (1989) The near-tip field at high crack velocities. *Int. J. Fract.* **39**(1–2), 1–13.

Broberg, K. B. (1994) Intersonic bilateral slip. Private communication.

Brock, L. M. (1977) Two basic problems of plane crack extension: a unified treatment. *Int. J. Engng Sci.* **15**, 527–536.

Brock, L. M. (1979) Rapid interface flaw extension with friction—I. Basic analysis. *Int. J. Engng Sci.* **17**, 49–58.

Brock, L. M. and Achenbach, J. D. (1973) Extension of an interface flaw under the influence of transient waves. *Int. J. Solids Struct.* **9**, 53–67.

Burridge, R., Conn, G. and Freund, L. B. (1979) The stability of a rapid mode II shear crack with finite cohesive traction. *J. Geophys. Res.* **85**, 2210–2222.

Bykovtsev, A. S. and Kramarovskii, D. B. (1989) Non-stationary super-sonic motion of a complex discontinuity. *Appl. Math. Mech.* **53**(6), 779–786.

Deng, X. (1992) Complete complex series expansions of near-tip fields for steadily growing interface cracks in dissimilar isotropic materials. *Engng Fract. Mech.* **42**(2), 237–242.

Freund, L. B. (1972) Energy flux into the tip of an extending crack in an elastic solid. *J. Elasticity* **2**, 341–349.

Freund, L. B. (1979) The mechanics of dynamic shear crack propagation. *J. Geophys. Res.* **84**, 2199–2209.

Freund, L. B. (1990) *Dynamic Fracture Mechanics.* Cambridge University Press, Cambridge.

Gol'dshtein, R. V. (1967) On surface waves in jointed elastic materials and their relation to crack propagation along the junction. *Appl. Math. Mech.* **31**, 496–502.

Lambros, J. and Rosakis, A. J. (1994a) Dynamic decohesion of bimaterials: experimental observations and failure criteria. *NSF/ONR Symp. Dynamic Failure of Modern Materials*, California Institute of Technology, 3–5 February 1994. (Also to appear in a special volume of the *Int. J. Solids Struct.* devoted to Dynamic Failure of Modern Materials, 1994.)

Lambros, J. and Rosakis, A. J. (1994b) On the development of a dynamic decohesion criterion for bimaterials. In preparation.

Lambros, J. and Rosakis, A. J. (1995) Shear dominated transonic crack growth in a bi-material—I. Experimental observations. *J. Mech. Phys. Solids* **43**(2), 169–188.

Liu, C., Lambros, J. and Rosakis, A. J. (1993) Highly transient elasto-dynamic crack growth in a bimaterial interface: higher order asymptotic analysis and optical experiment. *J. Mech. Phys. Solids* **41**(12), 1887–1954.

Simonov, I. V. (1983) Behavior of solutions of dynamic problems in the neighborhood of the edge of a cut moving at transonic speed in an elastic medium. *Mech. Solids (Mekhanika Tverdogo Tela)* **18**(2), 100–106.

Willis, J. R. (1971) Fracture mechanics of interfacial cracks. *J. Mech. Phys. Solids* **19**, 353–368.

Willis, J. R. (1973) Self-similar problems in elastodynamics. *Phil. Trans. R. Soc. (Lond.)* **274**, 435–491.

Wu, K. C. (1991) Explicit crack-tip fields of an extending interface crack in an anisotropic bimaterial. *Int. J. Solids Struct.* **27**(4), 455–466.

Yang, W., Suo, Z. and Shih, C. F. (1991) Mechanics of dynamic debonding. *Proc. R. Soc. Lond. A* **433**, 679–697.

Yu, H. and Yang, W. (1994) Mechanics of transonic debonding: the anti-plane shear case. Private communication.